Citizen radio science: an analysis of Amateur Radio transmissions with e-POP RRI

G. W. Perry[1], N. A. Frissell[2,*], E. S. Miller[3], M. Moses[2], A. Shovkoplyas[4], A. D. Howarth[1], and A. W. Yau[1]

[1]Department of Physics and Astronomy, University of Calgary.

[2]Bradley Department of Electrical and Computer Engineering, Virginia Polytechnic Institute and State University.

[3]The Johns Hopkins University Applied Physics Laboratory.

[4]Afreet Software.

[*]Now at Center of Solar-Terrestrial Research, New Jersey Institute of Technology.

Corresponding author: Gareth Perry (perry@phys.ucalgary.ca)

Key Points:

- Amateur Radio transmissions are used to detect plasma cutoff and single-mode fading
- Fundamental ionospheric characteristics and magnetoionic phenomena can be studied with Amateur Radio transmissions
- New and compelling radio science experiments are possible with the participation of citizen radio scientists

Abstract

We report the results of a radio science experiment involving citizen scientists conducted on 28 June 2015, in which the Radio Receiver Instrument (RRI) on the Enhanced Polar Outflow Probe (e-POP) tuned-in to the 40 and 80 m Ham Radio bands during the 2015 American Radio Relay League (ARRL) Field Day. We have aurally decoded the Morse coded call signs of 14 Hams (amateur operators) from RRI's data to help ascertain their locations during the experiment. Through careful analysis of the Hams' transmissions, and with the aid of ray tracing tools, we have identified two notable magnetoionic effects in the received signals: plasma cutoff and single-mode fading. The signature of the former effect appeared approximately 30 seconds into the experiment, with the sudden cessation of signals received by RRI despite measurements from a network of ground-based receivers showing that the Hams' transmissions were unabated throughout the experiment. The latter effect, single-mode fading, was detected as a double-peak modulation on the individual "dots" and "dashes" of one the Ham's Morse coded transmissions. We show that the modulation in the Ham's signal agrees with expected fading rate for single-mode fading. The results of this experiment demonstrate that Ham Radio transmissions are a valuable tool for studying radio wave propagation and remotely sensing the ionosphere. The analysis and results provide a basis for future collaborations in radio science between traditional researchers in academia and industry, and citizen scientists in which novel and compelling experiments can be performed.

Plain Language Summary

We report the results of an experiment in which we used a satellite-based radio receiver to eavesdrop on Ham radio communications as the satellite passed over the United States. We identified 14 Ham radio users by their call signs, and used this information to determine their location during the experiment. We were able to identify unique signatures in the Hams' signals that are directly related to the nature of the how the Hams' radio waves traveled through the Earth's ionosphere up to the satellite. Furthermore, we used our knowledge of the position of the spacecraft, and the location of the Hams and their broadcast frequencies to deduce the structure of the Earth's ionosphere over the United States during the experiment. This experiment and its results show that Ham radio transmissions and Hams (amateur radio operators) can be valuable assets in determining the structure of the ionosphere over large geographic regions.

1 Introduction

1.1 Citizen science and ham radio

In recent years, citizen science, the participation and collaboration of the general public in scientific activities carried out by formally trained and accredited scientists, has become a popular avenue for increasing the efficiency and diversity of scientific methodologies, and for augmenting the general public's awareness of the subject matter under investigation. This is especially true in solar-terrestrial science [*Knipp,* 2015], which has a number of young, active citizen science projects underway that engage thousands of public participants. Examples of successful citizen science projects include the Solar Stormwatch [*Barnard et al.,* 2014], which relies on public participation to analyze the STEREO spacecraft's extensive database and study solar coronal mass ejections (CME), and the Aurorasaurus project [*MacDonald et al.,* 2015, 2018] which enables the general public's participation via a web portal and mobile phone application to report sightings of the aurora borealis and australis.

The focus of this work is on radio transmissions from Amateur Radio enthusiasts. The Amateur Radio community (also known as the "Ham" community, whose members are hereafter referred to as "Hams") has also been active in citizen science projects. As of October, 2017, there are an estimated 745,000 registered Ham Radio operators in the United States (cf. www.arrl.org/fcc-license-counts), an increase from approximately 733,000 in 2015. Citizen radio science projects aim to leverage the prevalence of Hams, their transmissions, and expertise to provide additional scientific insight into radio wave propagation and the nature of the ionosphere.

There are examples of Hams actively participating in science experiments dating back several decades. In one case, *Gerson* [1955] relied on a distributed network of Hams to detect and infer the movement of sporadic-E layers, noting "the cooperation and enthusiasm of this group exceeded all expectations, and the fact that worthwhile results were obtained is a tribute to their perseverance and conscientiousness". This strong relationship continues today. The Ham Radio Science Citizen Investigation (HamSCI) organization [*Silver*, 2016], has been a focal point for organizing and coordinating Hams "to advance scientific research and understanding through Amateur Radio activities" (cf. www.hamsci.org). One example of these efforts and their utility is reported in *Frissell et al.,* [2014], which showed that a Ham Radio reporting network, the Reverse Beacon Network (RBN) (www.reversebeacon.net), could be used to study the effects of a solar flare on radio wave propagation in the North American sector.

Ham Radio operators have also worked to support scientific spacecraft missions. The Radio Aurora Explorer (RAX) and RAX-2 space science satellite missions [Bahcivan and Cutler, 2012; Bahcivan et al., 2014] used the Ultra High Frequency (UHF) Ham radio band and Hams as receiver stations for data downlinks, while the Cal Poly (California Polytechnic State University) PolySat program [Puig-Suari et al., 2001] also worked with the Ham Radio community to design the spacecraft and ground communications infrastructure for their missions.

In this work, we present results from a radio science experiment on 28 June 2015, which was organized with HamSCI and made successful with the help of the American Radio Relay League (ARRL) (www.arrl.org). This experiment involved the active participation of citizen scientists, i.e., Hams, and the Radio Receiver Instrument (RRI) on-board the CAScade, Smallsat and Ionospheric Polar Explorer (CASSIOPE) spacecraft. In the experiment RRI successfully recorded the transmissions of several Hams. We used this information to identify the Hams and confirm their location and the geographic origin of their transmissions. An assessment of the Hams' signals reveals two magnetoionic phenomena: plasma cutoff and single-mode fading.

1.2 Remote sensing of the ionosphere's critical frequency

By detecting and monitoring the Hams' transmissions, we were able to infer the critical frequency of the nighttime ionosphere over the North American sector during the period of the experiment. In essence, the experiment was a plasma frequency cutoff experiment in which the cutoff effect was a manifestation of the "secant law" [*Levis et al.,* 2010]: the product of the ionospheric plasma profile and the complement of elevation angle between the Hams' locations and CASSIOPE. The secant law is commonly associated with ionospheric sounders, which have been operated both on the ground as ionosondes [*Breit and Tuve*, 1925], and from orbital altitudes, for example, on the Alouette 1 spacecraft [*Warren*, 1963]. The sounding technique relies on the fact that the index of refraction of an electromagnetic wave in the ionosphere's magnetoplamsa is a function of the plasma frequency. A vertically propagating radio wave with a frequency that is less than the peak plasma frequency of the ionosphere (the critical frequency) will be reflected; the ionosphere's transmissivity goes to zero. The critical frequency can be inferred by determining the radio frequency at which incident radio waves are no longer reflected. The same principle applies to sounders in orbit; however, they are usually situated above the bulk of the ionospheric density and direct their transmissions vertically downward.

For a radio receiver in orbit, one can infer the critical frequency of the ionosphere with a technique that is the complement of the sounding technique. By monitoring a signal at a fixed frequency and the angle subtended between the receiver and transmitter, the angle at which signal cutoff is detected (when the transmitted signal can no longer propagate through the ionosphere to the receiver) can be used to infer the ionosphere's critical frequency.

1.3 Magnetoionic effects on propagating radio waves

We also report the detection of the interference pattern of one Ham's signal, which was generated by the superposition of non-parallel transmitted wave fronts at CASSIOPE's location. These signatures can manifest as sporadic decreases in signal amplitude, also known as "fades", detected by a radio receiver. Detecting and analyzing signal fades and scintillations is an important aspect of studying radio wave propagation and the morphology of the ionospheric medium.

Seminal work in studying fading and scintillations in the High Frequency (HF) regime include *James* [2006] and *James et al.* [2006]. They analyzed fades detected by the International Satellites for Ionospheric Studies (ISIS) 1 and 2 spacecraft. They found that the majority of fades were attributed to Faraday rotation, wherein the orientation angle of a linearly polarized propagating wave, a superposition of a circularly polarized ordinary mode (O-mode) component and oppositely circularly polarized extraordinary mode (X-mode) component, rotates as it propagates through the ionosphere due to the mismatch between the rotation rates of the O- and X-modes. The mismatch in rotation rates is a result of the birefringent properties of the ionosphere. As the linearly polarized wave rotates, its electric field becomes orthogonally oriented with respect to a satellite receiver antenna, producing an abrupt decrease in signal power on the receiver system – hence, a fade.

James [2006] and *James et al.* [2006] also studied other, more infrequent fades in the ISIS data. They reported "single-mode" fades, which are different from Faraday fades: unlike Faraday fades, the single-mode fades only occur to either the O- or X-mode components of a wave, and not the combined (linear) mode. The single-mode fades are a signature of self-interference patterns which can setup as a result of variations in the phase paths of rays which make-up the phase front of a transmitted signal (we are invoking the ray optics perspective here). As a result, non-parallel rays interfere and setup constructive and destructive interference patterns in the ionosphere.

The single-mode fades are measured as the satellite's radio receiver passes through the troughs of a destructive interference pattern associated with an individual propagation mode, e.g., the O-mode. *Perry et al.* [2017] also reported the detection of single-mode fades of radar pulses measured with RRI. The phase path variations responsible for self-mode fades are setup by plasma density irregularities whose plasma density gradients alter the phase paths of individual rays that make up the phase front. Therefore, self-mode fades are a phenomenon which can be used to study the small-scale morphology of the ionosphere.

2 The 2015 e-POP RRI Field Day experiment

2.1 e-POP RRI

The Radio Receiver Instrument (RRI) [*James et al.,* 2015] is one of eight instruments that make up the Enhanced Polar Outflow Probe (e-POP) on the CASSIOPE spacecraft [*Yau and James*, 2015], which was launched into a 325 to 1500 km, 81° inclination orbit, on 29 September 2013. RRI's scientific objectives include studying HF radio wave propagation in the terrestrial ionosphere, as well as the influence of F-region plasma density structures on radio wave propagation.

RRI is a digital receiver with four, 3-m monopole antennas. Figure 1 depicts RRI on CASSIOPE while the spacecraft is a "nadir" orientation and RRI's boresite is parallel to the spacecraft's ram direction. The three-axis stabilized CASSIOPE spacecraft allows for the RRI boresite to be directed at will, including slewing to a fixed ground target.

RRI has a tuning range between 10 Hz and 18 MHz. It performs quadrature sampling at 62.5 kHz, and passes the digitized signal through a 30 kHz (nominal) passband filter. We direct the reader to *James et al.,* [2015] and *Perry et al.,* [2017] for more information on its other capabilities. RRI's data is recorded on two channels, Inputs A and B. Under normal operations, Input A is the addition of inputs from RRI Monopole 1 and 2, forming Dipole 1, and Input B from Monopoles 3 and 4, forming Dipole 2. Each dipole may be tuned to a different frequency. For example, RRI Input A may be tuned to 4 MHz while RRI Input B is tuned to 40 kHz. This flexibility allows RRI to study a wide variety of HF radio emissions, including those produced artificially by ionospheric heaters [*James et al.,* 2015, 2017] and over-the-horizon radar systems [*Burrell et al.,* 2015; *Perry et al.,* 2017, *Burrell et al.*, 2018].

2.1 Ham Radio operators and the 2015 ARRL Field Day

Ham Radio users are Amateur Radio enthusiasts who are licensed by their respective national organizations. The ARRL is the largest Ham Radio organization in the United States, representing 100,000 members throughout the United States and elsewhere throughout the world. Every year, the ARRL organizes a "Field Day" in the United States and Canada. The purpose of Field Day is to encourage Ham Radio users to venture into the field and hone their skills "off the grid". In essence, Field Day is a large emergency preparedness exercise: Ham users are practicing their ability to manage the wireless communications infrastructure in the event of a national emergency or natural disaster.

The transmissions that make up communications between Hams are encoded with information – the Hams' call signs – that can be used to uniquely identify the participants and their geographic locations. Therefore, during a Field Day contest in which the objective is to make as many contacts as possible, the CW amateur band is full of transmissions encoded with information identifying the Hams and their location. From an HF radio wave science perspective, a Field Day contest provides a unique opportunity to conduct an HF radio science experiment featuring multiple, geographically distributed HF sources that can be recorded with a receiver, e.g., RRI. Analysis of the received signal can then be used to constrain HF ray tracing simulations, to provide insight into the structure and state of the ionosphere during the experiment.

2.3 The 2015 e-POP/ARRL Field Day Experiment

The 2015 e-POP ARRL Field Day experiment took place between 01:16:14 and 01:18:14 UT on 28 June 2015. At the time, the CASSIOPE spacecraft was over the continental United States (357 – 386 km altitude), traveling along a southeasterly trajectory. CASSIOPE's ground track during the experiment is plotted in Figure 2, along with the locations of the Ham users identified in RRI's data (which is discussed in more detail below), and contour lines (dashed traces) of the ionosphere's plasma frequency at 271 km altitude according to the International Reference Ionosphere (IRI) 2016 [Bilitza et al., 2017].

e-POP RRI's Input A was tuned to 3.525 MHz (80 m band), while Input B was tuned to 7.025 MHz (40 m). Throughout the experiment, CASSIOPE was kept in the nadir orientation; that is, CASSIOPE's **x** axis was parallel to the ram direction while its **z** axis was pointed to nadir (see Figure 1); the spacecraft's spin rate was ~0. CASSIOPE's orbit placed it over the North American sector several times throughout the Field Day contest; however, due to the limited telemetry bandwidth, RRI could only be activated for a few minutes.

To maximize the likelihood of intercepting Ham Radio transmissions, we selected the orbit closest to the time when the 40 and 80 m bands were expected to have the most activity: near local dusk on the Saturday night (28 June) of the Field Day weekend. The motivation was to tune RRI to both amateur bands instead of only one, even though the carrier frequency of the longer wavelength band, 80 m (3.525 MHz), was below the critical frequency expected for the ionosphere during the experiment. We also published an announcement on the ARRL website in the days leading up to the Field Day, that outlined the experiment and RRI's tuned frequencies, and encouraged Hams to transmit on those frequencies so that their transmissions might be received by RRI.

3 Observations and Analysis

3.1 2015 Field Day observations

An RRI spectrogram of the Field Day experiment is given in Figure 3. We are only showing data from Input B (monopoles 3 and 4 combined), which was tuned to 7.025 MHz. No signal was detected in Input A, and therefore it is not shown. The spectrogram in Figure 3 was generated using discrete Fourier transforms with a Blackman-Harris window of 12,000 samples (192 ms temporal resolution) and a 6000 sample overlap between transforms. Ham radio transmissions are easily identified as short and narrow bursts of intensity in the Input B data plotted in Figure 3. These transmissions were on the 40 m Ham band.

At approximately 7.029 MHz, there is a CW signal that lasts the entire duration of the experiment. We could not identify the signal or its origin. We do not believe it is a Ham signal. Similar unidentified signals are often seen with RRI, and are generally classified as "noise" until they can be identified. Additionally, just prior to 01:17:54 UT, both bands (Inputs A and B) recorded a diffuse and broadband signal. We are unsure as to its origin. We could not identify the signal as a Ham signal, however, we could not rule-out that possibility either. This will be discussed in a little more detail shortly.

Transmissions from the Field Day were recorded across RRI's entire Input B band. Since RRI performs quadrature sampling at 62.5 kHz, it is able to record signal in the 7.025 MHz ± 31.25 kHz band [Brigham, 1988]. According to specifications, RRI uses a 30 kHz passband filter [James et al., 2015]; therefore, only signal in the 7.025 MHz ± 15 kHz band should be present. However, as Figure 12 in *James et al.,* [2015] shows, the passband is in reality closer to 40 kHz wide, meaning that RRI should have been able to record signals on the 7.025 ± 20 kHz band, a significant portion of the 7 MHz CW band. Indeed, as Figure 3 shows, several CW signals were received between 7.005 and 7.045 MHz. This is an important observation as it shows that RRI is able to detect weak transmitters (compared to other ground-based systems such as radars), even on the edges of its passband filter. Beyond those frequencies the effectiveness of the passband filter is evident – Input B's signal is suppressed.

3.1 Identification of Ham Radio signals

In order to confirm that the signal recorded by Input B originated from Ham Radio operators participating in the Field Day, RRI's signal was converted to audio format and decoded in two ways. First, the data was fed into a software program *CW Skimmer* (www.dxatlas.com/cwskimmer), a multi-channel CW decoder and analyzer. An audio file from each of RRI's inputs recorded during this experiment is provided as supplementary information S1 and S2.

The program has some success at decoding call signs from the received Morse coded signals; however, due to signal scintillation and degradation (a byproduct of the signals' interaction with the terrestrial ionosphere) the skimmer's results had to be confirmed and supplemented aurally. Decoding the signals in this way is a cumbersome task and would not be practical for similar experiments performed on a larger scale, with more Hams involved. For those experiments, novel analysis techniques would be required to automate the process. Indeed, software such as CW Skimmer could be modified for analyzing RRI's band, or statistical analysis methods could be implemented that could allow for accurate results using only the registered location of the Hams.

Figure 4 shows an example of a Morse coded signal that was received by RRI. The intensity of the signal during the first five seconds of the Field Day experiment, measured by RRI in the 7.0334 – 7.0335 MHz range (filtered by an 800-sample Blackman-Harris window with a 400-sample overlap) is plotted. Starting shortly after 01:16:14.5 UT, dots and dashes (in Morse code) spell out 'K9ESVFD'. The first five letters, 'K9ESV', correspond to a Ham Radio user who was located at 42.34°N, 88.44°W (geographic coordinates) just northwest of Chicago, Illinois. The next two letters "FD" are for "Field Day", since the Ham user was participating in the ARRL Field Day activities.

In total, the call signs of 20 Ham Radio Field Day participants were decoded from the signals received on RRI's Input B. Two Ham Radio call sign lookup services, *QRZ.com* and *ARRL.org*, along with Google's search tool were used to identify the operators and clubs associated with each call sign and obtain their contact information. Of the original 20 call signs decoded, we were able to make contact with 14 of the Hams after the experiment.

Not only is each call sign associated with a Ham Radio operator or club, it is also associated with a geographic location – the location of the operator or club. However, since the ARRL Field Day encourages participants to travel outside of their home area and operate off the grid, each identified operator was asked to confirm their location during the experiment. Table 1 summarizes the identified operators, the frequency they were recorded on by RRI, and the geographic origin of their transmissions. Additionally, the locations of each Ham operator at the time of the experiment is also plotted (in blue) in Figure 2.

In addition to those operators recorded by RRI, the location of an operator who was recorded transmitting in RRI's band by a ground-based receiver network, the RBN, but not recorded by RRI was also confirmed. This information was used as a "null case" in our analysis. The Ham's location, W1HP, is marked red in Figure 2 and Table 1. More details on the null case and the RBN and its use in this analysis will be discussed shortly.

Call Sign	Geographic Latitude (°)	Geographic Longitude (°)	Frequency (MHz)
W9NE	41.90	-88.49	7.00949
K8CAD	44.22	-85.40	7.01138
W9PN	42.72	-89.03	7.01168
W9MVA	43.87	-91.18	7.01453
W9TE	41.13	-85.09	7.02227
W9JP	39.87	-86.04	7.02676
W9SW	41.84	-87.81	7.02676
K9EAM	44.46	-88.09	7.0325
K9ESV	42.34	-88.44	7.03349
K8SCH	39.19	-84.72	7.0361
N9SAB	42.36	-87.83	7.03905
K8ED	42.65	-83.51	7.04339
K9OR	42.21	-87.85	7.04483
K2MK	39.94	-74.88	7.04483
W1HP	42.69	-71.22	7.006

Table 1: A list of each Ham user that was identified in RRI's data, their geographic location, and their transmitting frequency. Each Ham was contacted to confirm their location during the experiment. W1HP (red) was not identified with RRI, but was recorded by RBN, transmitting in RRI's operational band during the experiment.

3.2 Analysis of the received signals

3.2.1 Disappearance of the Ham transmissions

One of the more prominent features of the data received on Input B during the Field Day experiment is the cessation of transmissions received approximately 30 seconds after the start of the experiment. CASSIOPE's location when this occurred is marked with a black star in Figure 2. An inspection of Figure 3 shows that this occurred across the entire band. We confirmed that both the RRI instrument and the spacecraft were operating nominally at the time of the experiment. One of two things happened: either all of the Hams recorded in the first 30 seconds of the experiment stopped transmitting and kept silent for the remainder of the experiment, or their transmissions were cut-off after the 30 second mark of the experiment by some other intermediary.

To address the first hypothesis, we inspected the records of the RBN, a globally distributed network of passive radio receivers that decode and log radio transmissions in the Ham bands. RBN software decodes the Morse coded transmissions in order to identify the Ham user associated with them. Figure 5 shows a plot of some of the call signs identified by RBN between 01:12:00 and 01:18:00 UT (in one minute increments) during the experiment, and their estimated propagation paths between the Ham and RBN receiver. It shows that the level of activity remained relatively constant before, during, and after the RRI Field Day experiment. This includes activity from call signs recorded by RRI (see Figure 5f): W9TE (yellow), W9JP (red), and K9ESV (violet). Therefore, the disappearance of signal in Figure 3 was not due to a cessation of transmissions by Field Day participants.

Our second hypothesis is that the Ham transmissions were cut-off by another intermediary: the ionosphere. Insight into the state of the ionosphere during the experiment are provided by ionosondes at Boulder, Austin, and Millstone Hill. This information is shown in Table 2. The critical frequency of the ionosphere (foF2) west and east of CASSIOPE's track was slightly below the frequency band used in the Field Day experiment, but above the frequency band south of the experiment track. CASSIOPE's altitude was above the altitude of the ionosphere's peak plasma density (hmF2) during the experiment. It is therefore plausible that the cessation in transmissions received by RRI are a result of plasma cutoff.

Ionosonde location	**Geographic Latitude (º)**	**Geographic Longitude (º)**	**foF2 (MHz)**	**hmF2 (km)**	**Measurement time (UTC)**
Boulder	40.0	-105.3	6.875	268	01:20:05
Austin	30.4	-97.7	8.250	310	01:20:05
Millstone Hill	42.6	-71.5	6.713	285	01:20:00

Table 2: Ionospheric plasma density information obtained from ionosonde measurements in the vicinity of CASSIOPE's track during the Field Day experiment. This information was retrieved from www.ndgc.noaa.gov.

To explore this hypothesis further, we conducted a ray trace simulation using the (Provision of High-frequency Raytracing Laboratory for Propagation studies) PHaRLAP ray tracer [Cervera and Harris, 2014]. The PHaRLAP code produces 3D ray trace solutions through an input ionosphere. We chose to use the 2016 IRI ionosphere [Bilitza et al, 2017], with foF2 and foE constrained to 7.00 and 2.31 MHz, respectively, to reflect the ionosonde measurements from Boulder and account for the fact that a positive meridional gradient in foF2, directed towards geographic south, would have been present at the time. We chose to adjust IRI's parameters to reflect the ionosonde data since IRI underestimated the value of foF2 during the experiment.

It is important to note that by constraining IRI's foF2 parameter, foF2 is fixed to a single value over the entire region, and any meridional or zonal foF2 gradients that would have existed in reality are not reproduced by IRI in this case. In this instance, the regional foF2 zonal and meridional gradients are relatively small: IRI (without a fixed foF2) predicts a meridional gradient of ~0.075 MHz/°, directed geographically southward, in the region of interest. The Boulder and Austin ionosonde measurements indicate a gradient approximately twice as large.

We launched rays originating from each location listed in Table 1 at their corresponding carrier frequencies. The rays were launched from each source in 1.26° elevation angle increments, over the range of 0.5° to 90°, and 5.05° increments in bearing, over the range of 0° to 360°. In total, 5040 rays were simulated for each station. We were limited in our elevation and bearing angle resolution by computer memory. Both the O- and X-propagation-modes (hereafter we will drop "propagation" for brevity) of the waves were considered; however, only the former will be discussed here. Our ray trace simulations indicate that X-mode rays were unable to penetrate the ionosphere in all cases (not shown).

The results of the ray trace simulation are given in Figure 6, which is a reproduction of Figure 2. Pierce point HF rays passing through CASSIOPE's altitude range during the experiment are plotted in magenta for all of the Ham stations identified, except for K2MK, which is plotted in cyan, and W1HP, which is plotted in red. The top panel in Figure 6 show 0.5 hop rays. These rays are those which propagate directly through the ionosphere to CASSIOPE's altitude. The bottom panel shows both 0.5 hop and 1.5 hop rays. The latter are rays which have undergone one internal reflection from the ionosphere and an additional reflection off the surface of the Earth. After the second reflection, the 1.5 hop rays were able to penetrate through the bottom-side ionosphere.

In Figure 6, it is evident that the region in which the Ham's transmissions were able to penetrate the ionosphere and propagate up to the spacecraft was isolated. This is especially clear in Figure 6a, where the transmission "iris" of the majority of the Ham stations overlaps a region encompassing the first half of CASSIOPE's track during the experiment. We also ran simulations with larger foF2 values. We found that each station's iris varied significantly with small changes in foF2. An IRI ionosphere with a uniform foF2 of 7.0 MHz offered the best reproduction of the signal cutoff measured by e-POP RRI during the experiment.

An unmodified IRI ionosphere, that is, the default IRI output which included meridional and zonal plasma density gradients, underestimated foF2 measured at Boulder and Millstone Hill, and produced large transmission irises that were inconsistent with RRI's measurements. Meanwhile, modified IRI ionospheres with foF2 values above 7.0 MHz produced irises that were restricted to a small region around each Ham station, which was also inconsistent with RRI's measurements. Therefore, we conclude that, in the vicinity of CASSIOPE's track, foF2 was ~7.0 +/- 0.1 MHz during the Field Day experiment. This estimate is crude, but it is still informative. The measurement indicates that the foF2 was higher than the foF2 measured at Boulder, confirming the presence of a meridional gradient in this ionospheric characteristic that is larger in the south than in the north, as expected.

The ray trace simulation results in Figure 6a support the second hypothesis for the cessation of Ham transmissions received by RRI. Only transmissions with elevation angles that were close to vertical were able to propagate through the ionosphere. Waves that were not vertically incident on the ionosphere were internally reflected. Since the transmission frequencies were very close to foF2, only a small angle of incidence was required to achieve internal reflection. This is an application of the *Secant Law* [Levis et al., 2010], wherein the effective critical frequency of the ionosphere is proportional to the secant of a radio wave's angle of incidence. Naturally, this effect is ideal for Ham Radio communications since internal reflection extends the operational range of a Ham Radio system.

During the Field Day experiment, as CASSIOPE moved south, Ham transmissions at lower elevations were not able to penetrate the ionosphere and propagate to RRI, hence the cessation in frequencies after approximately 01:16:44 UT. The ray trace simulation predicts that RRI should have observed signals up to 01:17:10 UT. The difference in time can be attributed to uncertainty in the structure of the ionosphere. By inspection of Figures 2 and 4 and Table 1, one can see that the longest lasting signals corresponded to Hams located almost directly under CASSIOPE's track. Those Hams would have the highest elevation angle with respect to the spacecraft. Hams with much lower elevation angles were cutoff sooner.

On the other hand, Figure 6b indicates that RRI should have detected 1.5 hop transmissions from the listed Hams. This may have been the case; however, the strength of those transmissions may have been too weak to be detectable by RRI. The ray trace simulation assumes that the surface of the Earth has a reflection coefficient that is unity, which is likely not true. The sparsity of points introduced by the 1.5 hop propagation mode shows that the likelihood of RRI receiving these transmissions would have been significantly lower than the 0.5 hop propagation mode. Therefore, the transmissions received by RRI during the experiment are most consistent with the 0.5 hop propagation mode. The diffuse signal appearing in Figure 3 just after 01:17:44 UT could be evidence of 1.5 hop propagation; however, we were unable to identify the signals, and thus, we could not distinguish them as a 1.5 hop propagation mode of the Hams identified in Table 1, a 0.5 hop propagation mode from other Hams, or other unidentifiable signals, such as an unrelated ground-transmitter or spacecraft noise.

We would now like to focus on the transmissions from K2MK and W1HP in Figure 6. The ray trace results suggest that neither transmission should have been received by RRI – neither cyan or red ray points appear west of 82° W. However, K2MK was recorded by RRI. Given the similar origin locations, operational frequencies, and having confirmed through the RBN and direct contact that W1HP was transmitting, we must ask why K2MK was detected by W1HP was not. This question is important for scientific reasons, as it addresses the level of complexity in the structure of the ionosphere.

It is evident that our model underestimates this complexity in the North American sector during the Field Day experiment. We hypothesize that the ionospheric structure has caused different propagation paths for these two Ham signals. Evidently, our model cannot reproduce the conditions under which K2MK's signal was able to propagate to RRI, while preventing W1HP's signal from doing the same.

During the first 30 seconds of the experiment, the elevation angle of RRI from K2MK and W1HP was approximately 9° and 13°, for a 0.5 hop propagation mode between the Ham and RRI, respectively. Given the ionospheric conditions at the time of the experiment, a multi-hop propagation mode is a likely scenario. The rays which would have undergone internal reflection would have continued as the signal propagated westward until it reached a location where the product of the ionosphere's critical frequency and the secant of the rays' incident angle allowed the rays to propagate through the ionosphere to RRI. However, our ray trace model does not support this. Transmissions from K2MK and W1HP internally reflect in perpetuity; K2MK does not penetrate through the ionosphere to be received by RRI (not shown).

To add to the complexity even further, Figure 2 indicates that meridional and zonal plasma density gradients should be expected at this time of day. This is consistent with the fact that the experiment took place near dusk, and the ionosonde data from Boulder, Millstone Hill and

Austin. Under these conditions, one would predict that W1HP's transmissions would be less likely to be internally reflected than K2MK's; however, as RRI's data shows, this was not the case. Ionospheric structures, such as a sporadic-E layer, may cause sufficient changes to propagation conditions that may have provided favorable propagation conditions to allow K2MK's signal to reach RRI; however, we could find no evidence of a sporadic-E layer in the Millstone Hill ionosonde data, which was taken in close proximity to both hams.

An alternative explanation for receiving K2MK's transmission and not W1HP's may be found in the Hams' equipment. K2MK's transmitter used an omni-directional ground antenna with a 1500 W power output. Meanwhile, W1HP used an inverted V antenna with a 100 W transmitter. Both transmitters had sufficient directionality towards RRI. This points to a scenario where both transmitters were able to propagate through the ionosphere up to RRI; however, since W1HP's transmitting power was much less than K2MK's, it may not have been strong enough to be detectable by RRI. By inspection of Figure 3, RRI's noise floor is approximately 10 dB below K2MK's signal strength. If we assume that both K2MK and W1HP have equivalent gain patterns, and that their transmissions experienced the same level of loss en route to RRI, W1HP's would be difficult to detect since its strength would be close to the noise floor – W1HP's transmitting power was ~12 dB lower than K2MK's.

This case study shows that our ray trace modeling, in its current form, is limited in its representation of HF transcontinental radio wave propagation close to the ionosphere's critical frequency. That is, the RRI data shows that complex HF propagation modes exist that cannot yet be explained. An improvement to our modeling could come from better understanding the role of signal strength. Currently, our ray trace simulations do not consider signal strength; however, they can be modified to do so. Phenomena which could cause a decrease in signal strength beyond geometric effects, such as absorption, could then be accounted for. Indeed, it is possible that W1HP's signal experienced stronger absorption than K2MK's signal, causing its signature to drop below the audible detection range. More information regarding a Ham's equipment, i.e., the power of their transmissions and their nominal radiation pattern would be ideal in this effort. Even though obtaining this information may be cumbersome on a case-by-case basis, it would be useful for gaining more insight into more complex HF propagation modes.

3.2.2 Signatures of magnetoionic physics in the Ham transmissions

Figure 7 presents one second of RRI data from Figure 5, which has been reprocessed with a 100 sample Blackman-Harris window. The pulses displayed correspond to the Morse code letters 'ES' and part of the dash in 'V'. Each pulse – a Morse code dot - exhibits substantial modulations in signal strength and is double-peaked with several, smaller-amplitude peaks superposed. The time separation between the double-peaks is consistently ~0.03 s, equivalent to a frequency of ~33 Hz, throughout the time segment. Based on our correspondence with K9ESV, we believe the signature is geophysical in origin rather than instrumental. Therefore, we wish to investigate the features as geophysical in origin.

One phenomenon that may account for the double-peaked signature in Figure 7 is multi-path propagation. More specifically, an interference pattern is established by the superposition of multiple O-mode wave fronts. A single-mode fade occurs when RRI passes through a region of destructive interference. Ray tracing simulations show that only the O-mode of K9ESV's transmissions is expected to penetrate the ionosphere.

In regions where multiple wave fronts with non-parallel wave vectors are present, regions of constructive and destructive interference will be established. This is described graphically in Figure 8, a reproduction of Figure 5 in *James et al.,* [2006]. Wave fronts with wave vectors $\boldsymbol{k_1}$ and $\boldsymbol{k_2}$, of equivalent wavelength, λ, are subtended by an angle α. A superposition of the wave fronts will generate planes of destructive interference, described by the dashed lines I_a and I_b in Figure 8, and a normal vector $\boldsymbol{N}$. The separation, d, between I_a and I_b, is given by:

$$d = \cos\left(\frac{\alpha}{2}\right)\frac{\lambda}{\sin\alpha}. \quad (1)$$

Assuming that the interference pattern setup is static, measurements by RRI while CASSIOPE moves through the area at an angle γ, measured with respect to $\boldsymbol{N}$, will intersect I_a and I_b at a rate of occurrence, F [*James et al., 2006*]:

$$F = \frac{2v\sin(\alpha/2)\cos\gamma}{\lambda}. \quad (2)$$

Evaluating Equation 2 with $v=7926\ ms^{-1}$, $\alpha = 15^\circ$ (derived by evaluating the ray tracing simulation results discussed earlier), $\lambda=40\ m$ and $\gamma=45^\circ$ gives $F = 36.6\ Hz$, which is in good agreement with the frequency of the double-peaked signature in Figure 7 (~33 Hz).

A value of $\gamma=0^\circ$ or $\gamma=90^\circ$ in Equation 2 is not likely given CASSIOPE's orbital track, which was almost directly due south with respect to K9ESV's location. Re-evaluating Equation 2 for $30^\circ \leq \gamma \leq 60^\circ$ gives $25\ Hz \leq F \leq 44\ Hz$, which is still in good agreement with what is observed in Figure 7. Since Figure 8 is a two-dimensional representation of a three-dimensional geometry, and the ray trace simulation solutions are estimates, it is difficult to justify a singular value for γ. Nonetheless, based on the ray trace simulation and our knowledge of CASSIOPE's orbit during the Field Day experiment we conclude that single-mode (O-mode) fading provides a plausible explanation for the double-peak modulation signature observed in Figure 7.

The double-peak modulation in Figure 7 is reminiscent of mode-splitting, also known as differential mode delay, wherein the O- and X-mode components of a transmitted signal become separated in time as a result of magnetoionic dispersion along the ray path. In a cold magnetoplasma, the X-mode of a propagating electromagnetic wave has a lower index of refraction and group velocity than the O-mode. This results in a time delay between modes when measuring the electromagnetic wave at a fixed point along the ray path.

To investigate the mode-splitting as a possible explanation for the modulation in Figure 7, we used PHaRLAP to generate ray traces corresponding to K9ESV's transmissions during the first second of the Field Day experiment for the same ionosphere investigated in Section 3.2.1. The ray trace solutions (not shown here) indicate that RRI likely only received the O-mode component of K9ESV's transmissions since the X-mode is more strongly affected by the ionosphere and was internally reflected. Therefore, the double-peak signature in Figure 7 is likely not due to mode-splitting, since only one mode – the O-mode – was incident on RRI. Both modes must be present for mode-splitting.

We also ruled-out Faraday fading as a possible explanation for the signatures in Figure 7. This effect is a manifestation of Faraday rotation. A peak voltage is measured by RRI whenever the electric field vector of an incident wave is aligned with the dipole. A minimum occurs whenever the electric field vector is at a right-angle with respect to the dipole. Hence, Faraday rotation would appear as an oscillation in signal strength in RRI's data. However, like mode-splitting, Faraday rotation requires both O- and X-mode components of the propagating electromagnetic wave to be present, which was not the case according to our ray trace simulations.

It is important to note that the IRI ionosphere used in our simulations is not identical to the measured ionosphere during the Field Day experiment. As such, there is a non-zero chance that the both the O- and X-modes were incident on RRI, and mode-splitting or Faraday fading could have caused the signatures in Figure 7. However, given previous measurements of these effects with RRI, e.g., Perry et al. [2017], we conclude that it is unlikely that this is the case.

4 Conclusions and Future Work

We have analyzed Ham Radio transmissions received by RRI on e-POP between 01:16:14 and 01:18:11 UT, during the ARRL Field Day experiment on 28 June 2015. We were able to aurally decode 14 Ham call signs, and confirm their geographic location during the experiment (listed in Table 1). An example of one Ham's transmissions, K9ESV, is shown in Figure 4.

The Hams' transmissions were only discernible for the first 30 seconds of the experiment even though the Hams continued to transmit throughout the duration of the experiment. We used the results of ray tracing simulations to show that the disappearance of the signals is an example of plasma cutoff and the secant law, wherein transmissions with lower elevation angles do not have a sufficient effective frequency to penetrate the ionosphere and are therefore internally reflected. Conversely, transmissions with higher elevation angles have a sufficient effective frequency to penetrate the ionosphere. The region where the radio transmissions are able to penetrate through the ionosphere is often referred to as the "iris" of accessibility [James et al., 2006]. This effect is graphically demonstrated in Figure 6, which shows that the majority of Ham transmissions received by RRI were almost directly below the CASSIOPE spacecraft during the first thirty seconds of the experiment.

We also examined the individual pulses and dashes of K9ESV's transmissions, which showed a clear modulation of ~33 Hz on each pulse and dash. The modulation produced a double-peak feature on the majority of K9ESV's transmissions. This signature is clearly identifiable in Figure 7. Noting that the modulation is not an instrumental effect, we explored three well-documented magnetoionic phenomena to explain the modulation: mode-splitting, Faraday fading, and single-mode fading. With the help of ray tracing simulations we were able to rule out the first two candidates. From our analysis, we concluded that single-mode fading, an effect that arises when RRI moves through the nulls of an interference pattern setup by the O-mode component of K9ESV's transmissions, is the most plausible explanation for the observed modulation. Our calculations show that single-mode fading should produce a "fading" signature in RRI's signal in a frequency range of 25 to 44 Hz, depending on CASSIOPE's trajectory and the propagation direction of the radio waves. This is in good agreement with the observed 33 Hz modulation observed on K9ESV's transmissions.

We have demonstrated the ability of Ham Radio enthusiasts to participate in insightful and compelling radio science experiments. By analyzing two minutes of data collected by e-POP RRI during the ARRL Field Day, we have shown that the Hams' transmissions can be used to detect and study fundamental magnetoionic processes that are key to radio wave propagation science, including the "iris" effect and single-mode fading.

The ability to detect and identify multiple Ham users within RRI's band provides the opportunity to conduct unique radio science experiments. Individually, the Hams' CW transmissions take up very little of the RRI bandwidth, allowing for several Hams to be recorded simultaneously. This makes it possible to coordinate citizen science experiments with the Ham community, involving a vast network of geographically distributed radio sources. Radio science experiments with multiple geographically distributed transmitters and a space-based radio receiver are rare and offer the potential to incorporate more advanced remote sensing techniques, such as tomography.

These experiments can also be coordinated with other citizen science initiatives, e.g., RBN, in conjunction with other ground-based instruments such as sounders and/or incoherent scatter radars to conduct a *full* analysis of radio wave propagation. We emphasize *full* since almost all ground-based radio science experiments are only able to sample a portion of the total energy transmitted, specifically, transmissions that are reflected by the ionosphere or scattered by ionospheric irregularities. Transmissions which penetrate through the ionosphere, such as the Ham signals received by RRI, are not (and cannot be) internally reflected once they have propagated past the altitude at which the critical frequency for that signal occurs. These signals are also unlikely to be scattered back to a ground receiver and are, therefore, inaccessible to them. However, by combining a ground-based network of transmitters and receivers, such as the Ham community and RBN, with a space based receiver such as RRI, one has the opportunity to analyze the radio energy that is reflected, scattered, and propagated through the ionosphere which provides a more comprehensive understanding of radio wave propagation.

This work provides a basis for future collaborations in radio science between researchers in academia and industry, and citizen scientists. Such collaborations will allow for radio wave propagation studies with multiple, geographically distributed transmitters and receivers, and a space based receiver – RRI, to provide unprecedented opportunities to remotely probe the ionosphere on a large scale, study its structure and dynamics, with the goal of generating new insight into radio wave propagation.

A follow-up citizen radio science experiment was performed during the 2017 ARRL Field Day, which lasted between 24 and 25 June 2017. For the 2017 Field Day, RRI was activated on five separate occasions, for approximately 10 minutes (50 minutes in total). Unlike the 2015 Field Day experiment, e-POP RRI's participation was heavily advertised. As a result, RRI's band was inundated with Ham Radio transmissions, necessitating new analysis techniques. The 2017 Field Day results illustrate the difficulty in scaling this type of experiment to larger scales. Aurally decoding hundreds of Ham radio signals and confirming their location origin is not practical, and therefore, novel analysis techniques will be required. The development of such technique and a thorough analysis of the 2017 Field Day results is currently underway. It is intended that e-POP will participate in all future ARRL Field Day events while CASSIOPE remains in orbit.

Acknowledgments, Samples, and Data

We acknowledge the support of the Natural Science and Engineering Research Canada (NSERC) Discovery Grant Program and Discovery Accelerator Supplement Program for this research, and the support of Canadian Space Agency (CSA) and MacDonald Dettwiller Associates (MDA) for e-POP mission and science operations. e-POP RRI data can be accessed at epop-data.phys.ucalgary.ca. We are grateful to Dr. Manuel Cervera, Defence Science and Technology Group, Australia, (manuel.cervera@dsto.defence.gov.au) for the HF propagation toolbox, PHaRLAP, which was used for the ray tracing simulations in this study. The authors acknowledge the use of IDL GEOPACK DLM in the production of the RRI data products used in this work. The authors also thank: Robert Gillies for his valuable discussions, the e-POP ESOC team: Greg Enno, Troy Kachor, Jamie Roberts, and Andrew White, for their valuable contributions to CASSIOPE operations, and the McHenry County Amateur Radio Emergency Service (ARES) and Radio Amateur Civil Emergency Service (RACES), also known as K9ESV, for their participation in this work. The authors also thank R. G. Gillies for their many fruitful discussions.

References

Bahcivan, H., and J. W. Cutler (2012), Radio Aurora Explorer: Mission science and radar system, Radio Sci., 47, RS2012, doi:10.1029/2011RS004817.

Bahcivan, H., J. W. Cutler, J. C. Springmann, R. Doe, and M. J. Nicolls (2014), Magnetic aspect sensitivity of high-latitude E region irregularities measured by the RAX-2 CubeSat, J. Geophys. Res. Space Physics, 119, 1233–1249, doi:10.1002/2013JA019547.

Barnard, L., et al. (2014), The Solar Stormwatch CME catalogue: Results from the first space weather citizen science project, Space Weather, 12, 657–674, doi:10.1002/2014SW001119.

Bilitza, D., D. Altadill, V. Truhlik, V. Shubin, I. Galkin, B. Reinisch, and X. Huang (2017), International Reference Ionosphere 2016: From ionospheric climate to real-time weather predictions, Space Weather, 15, 418–429, doi:10.1002/2016SW001593.

Breit, G., and Tuve, M. A. (1925), A Radio Method of Estimating the Height of the Conducting Layer. Nature, 116, 357, doi: 10.1038/116357a0.

Brigham, E. O. (1998), The Fast Fourier Transform and its applications, Prentice Hall, Upper Saddle River, New Jersey.

Budden, K. G. (1985), The Propagation of Radio Waves: The Theory of Radio Waves of Low Power in the Ionosphere and Magnetosphere, 1st ed., Cambridge Univ. Press, Cambridge, U. K.

Burrell, A. G., S. E. Milan, G. W. Perry, T. K. Yeoman, and M. Lester (2015), Automatically determining the origin direction and propagation mode of high-frequency radar backscatter, Radio Sci., 50, 1225–1245, doi:10.1002/2015RS005808.

Burrell, A. G., G. W. Perry, T. K. Yeoman, S. E. Milan, and R. Stoneback (2018), Solar influences on the return direction of high□frequency radar backscatter, Radio Sci., 53, 577–597, doi: https://doi.org/10.1002/2017RS006512.

Cervera, M. A., and T. J. Harris (2014), Modeling ionospheric disturbance features in quasi-vertically incident ionograms using 3-D magnetoionic ray tracing and atmospheric gravity waves, J. Geophys. Res. Space Physics, 119, 431–440, doi:10.1002/2013JA019247.

Frissell, N. A., E. S. Miller, S. R. Kaeppler, F. Ceglia, D. Pascoe, N. Sinanis, P. Smith, R. Williams, and A. Shovkoplyas (2014), Ionospheric sounding using real-time amateur radio reporting networks, Space Weather, 12, 651–656, doi:10.1002/2014SW001132.

Gerson, N.C. (1955), Sporadic E Movements, Journal of Metrology, 12, 74–80, https://doi.org/10.1175/1520-0469(1955)012<0074:SEM>2.0.CO;2.

Gillies, R. G., G. C. Hussey, G. J. Sofko, and H.G. James (2010), Relative O- and X-mode transmitted power from SuperDARN as it relates to the RRI instrument on ePOP, Ann. Geophys., 28, 861-871, https://doi.org/10.5194/angeo-28-861-2010.

Gillies, R. G., G. C. Hussey, G. J. Sofko, and H. G. James (2012), Modeling measurements of ionospheric density structures using the polarization of high-frequency waves detected by the Radio Receiver Instrument on the enhanced Polar Outflow Probe, J. Geophys. Res., 117, A04316, doi:10.1029/2011JA017457.

James, H. G. (2006), Effects on transionospheric HF propagation observed by ISIS at middle and auroral latitudes, Adv. Space Res., 38, 2303-2312, doi: 10.1016/j.asr.2005.03.114.

James, H. G., R. G. Gillies, G. C. Hussey, and P. Prikryl (2006), HF fades caused by multiple wave fronts detected by a dipole antenna in the ionosphere, Radio Sci., 41, RS4018, doi:10.1029/2005RS003385.

James, H. G., E. P. King, A. White, R. H. Hum, W. Lunscher, and C. L. Siefring (2015), The e-POP Radio Receiver Instrument on CASSIOPE, Space Sci. Rev., 189(1–4), 79–105, doi:10.1007/s11214-014-0130-y.

James, H. G., V. L. Frolov, E. S. Andreeva, A. M. Padokhin, and C. L. Siefring (2017), Sura heating facility transmissions to the CASSIOPE/e-POP satellite, Radio Sci., 52, 259–270, doi:10.1002/2016RS006190.

Knipp, D. J. (2015), Space weather and citizen science, Space Weather, 13, 97–98, doi: 10.1002/2015SW001167.

Levis, C. A., J. T. Johnson, and F. L. Teixeira (2010), Radio Wave Propagation: Physics and Applications, Wiley, Hoboken, New Jersey.

MacDonald, E. A., N. A. Case, J. H. Clayton, M. K. Hall, M. Heavner, N. Lalone, K. G. Patel, and A. Tapia (2015), Aurorasaurus: A citizen science platform for viewing and reporting the aurora, Space Weather, 13, 548–559, doi:10.1002/2015SW001214.

Macdonald, E. A., Donovan, E., Nishimura, Y., Case, N. A., Gillies, D. M., Gallardo-Lacourt, B., … Schofield, I. (2018), New science in plain sight: Citizen scientists lead to the discovery of optical structure in the upper atmosphere, Science Advances, 4, 16–21, doi: https://doi.org/10.1126/sciadv.aaq0030.

Perry, G. W., H. G. James, R. G. Gillies, A. Howarth, G. C. Hussey, K. A. McWilliams, A. White, and A. W. Yau (2017), First results of HF radio science with e-POP RRI and SuperDARN, Radio Sci., 52, 78–93, doi:10.1002/2016RS006142.

Puig-Suari, J., Turner, C., and W. Ahlgren (2001), Development of the standard CubeSat deployer and a CubeSat class PicoSatellite, IEEE Aerospace Conference Proceedings, 1, 347-153, doi: 10.1109/AERO.2001.931726.

Silver, W., HamSCI: Ham Radio Science Citizen Investigation (2016), QST, 100(8), 68–71, ISSN: 0033-4812.

Warren, E. S. (1963), Some Preliminary Results of Sounding of the Top Side of the Ionosphere by Radio Pulses from a Satellite. Nature, 197, 636, doi: 10.1038/197639a0.

Yau, A.W., and H. G. James (2015), CASSIOPE enhanced polar outflow probe (e-POP) mission overview, Space Sci. Rev., 189(1–4), 3–14, doi:10.1007/s11214-015-0135-1.

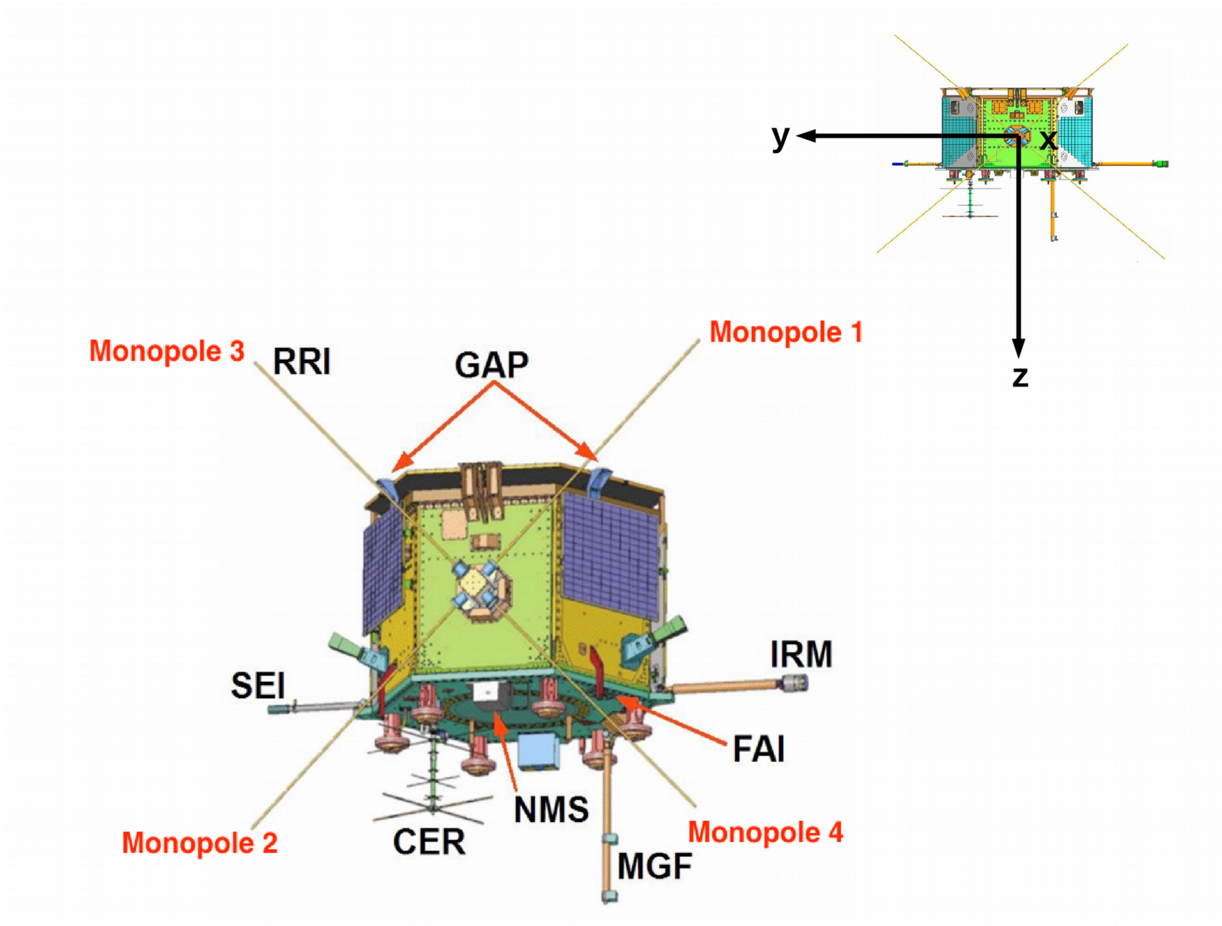

Figure 1: A diagram of the CASSIOPE spacecraft showing e-POP's eight instruments, reproduced from Perry et al., [2017]. RRI's four 3-m monopole antennas are labeled. The spacecraft coordinate system is shown on the inset.

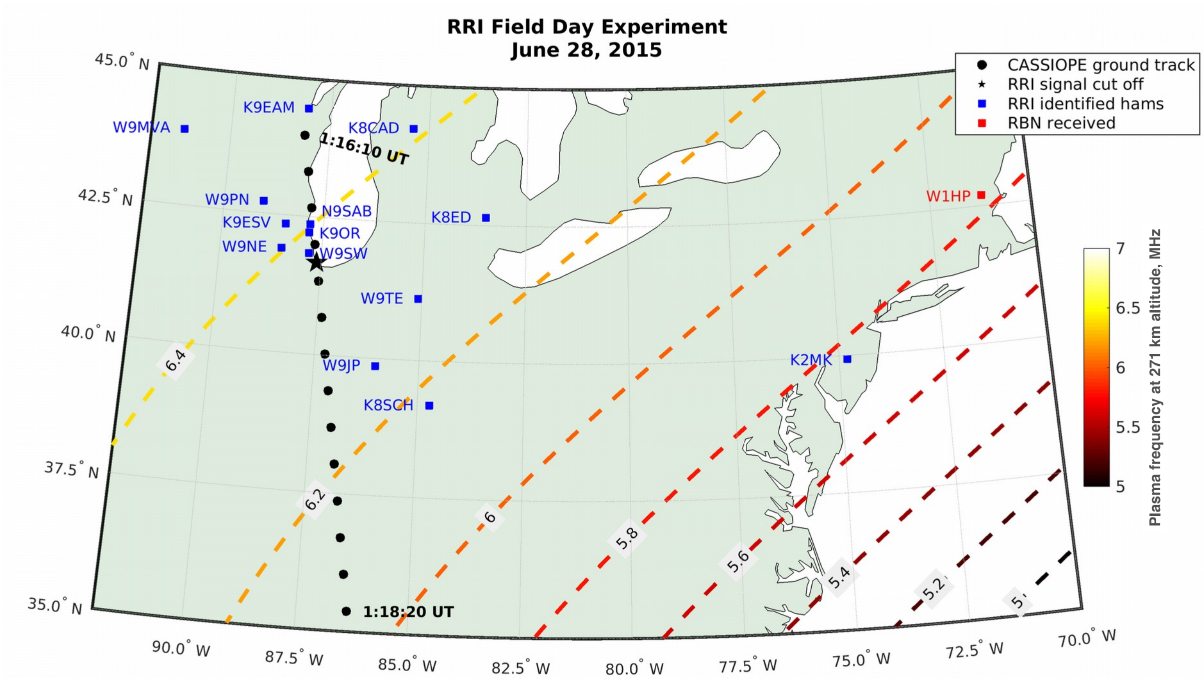

Figure 2: The ground track of the CASSIOPE spacecraft (black circles) between 01:16:10 and 01:18:20 UT, 28 June 2015. Also plotted are the locations of the hams identified in RRI's signal (blue squares) and described in Table 1. The red square marks the location of one ham user identified by the RBN but not identified in RRI's signal. The black star marks the approximate location along CASSIOPE's track at which RRI stopped receiving ham transmissions. Contours of the plasma frequency at 271 km altitude, derived from IRI 2016, are also plotted (dashed traces).

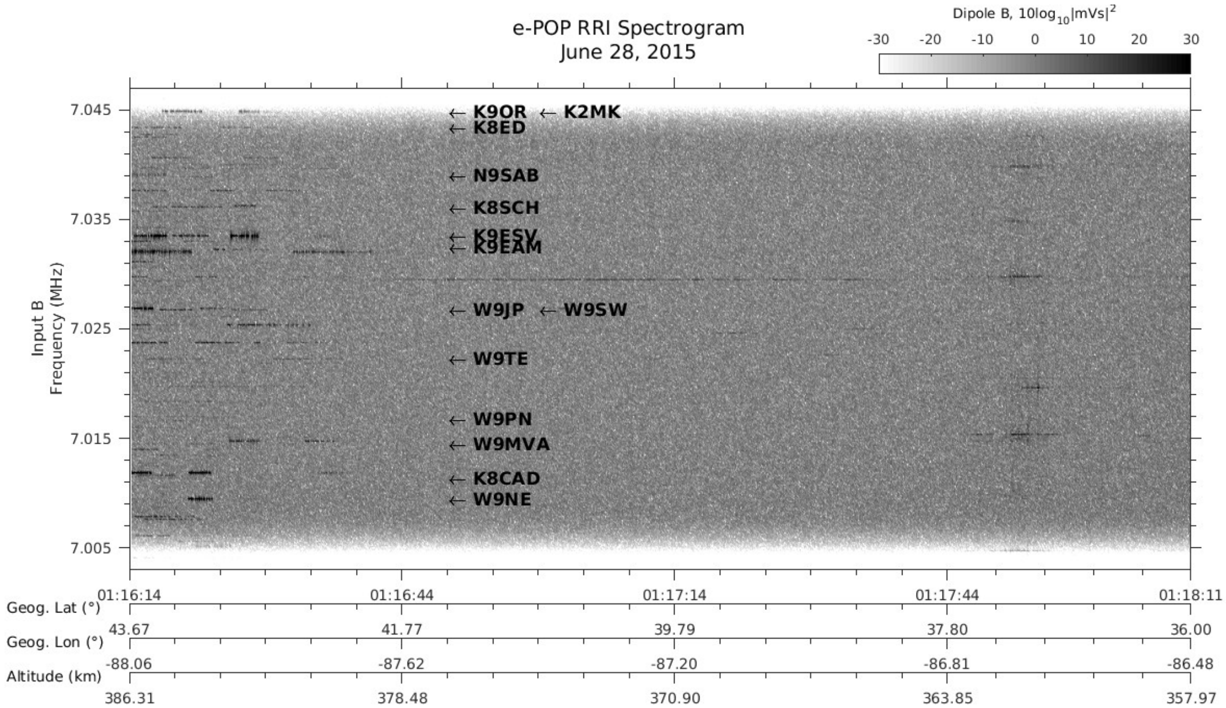

Figure 3: An RRI spectrogram for RRI Input B. Ham radio transmissions were received throughout the band. Identified Hams and their call signs are labelled. The effect of RRI's passband filter are clear: no ham signals were detected beyond 7.005 and 7.045 MHz. No ham signals were received after ~01:16:44 UT. The location corresponding to this time is marked with a black star in Figure 2.

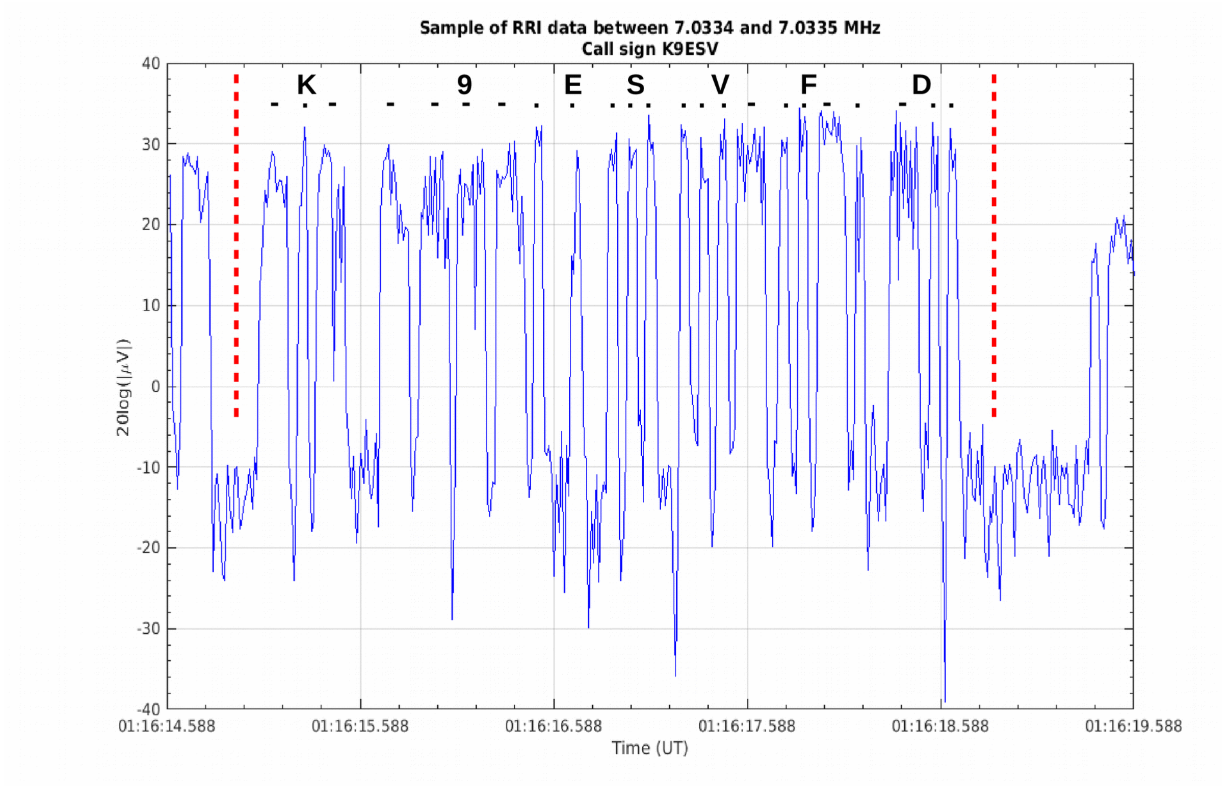

Figure 4: An excerpt of RRI's received signal between 7.0334 – 7.0335 MHz for the first five seconds of the Field Day experiment. The dots and dashes between the vertical red-dashed lines spell out K9ESVFD (in Morse code). K9ESV is the Ham's call sign, while FD is an abbreviation for "Field Day".

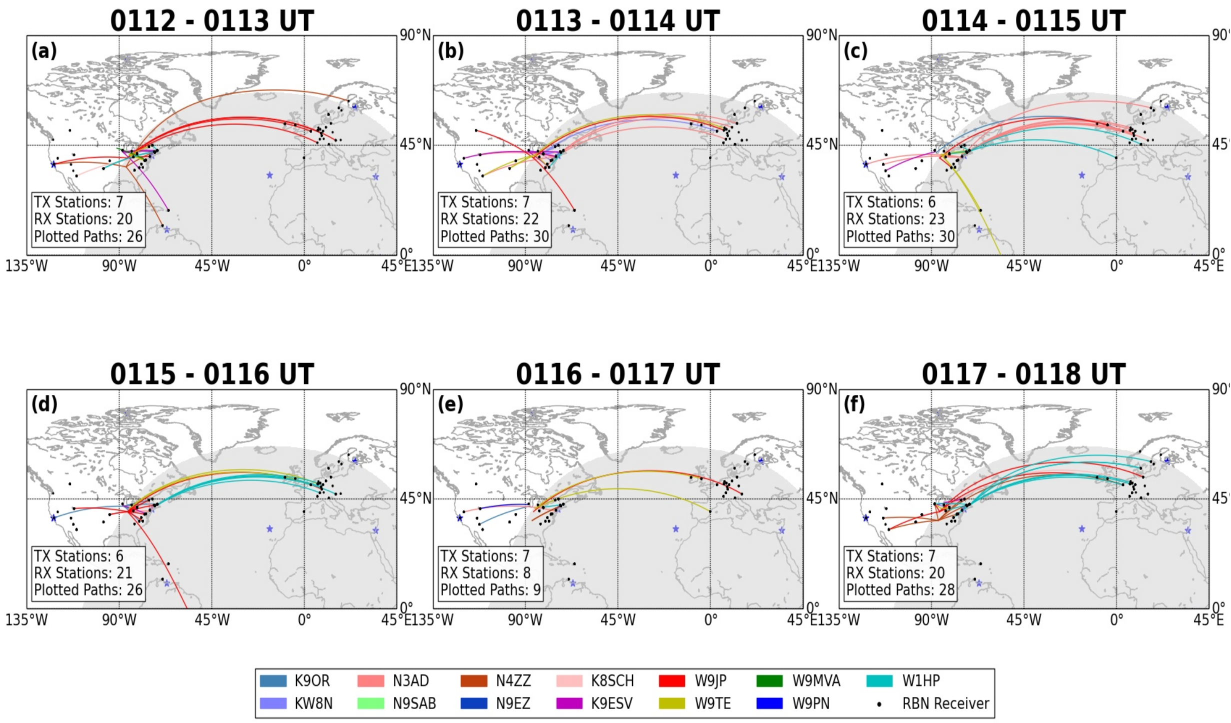

Figure 5: A visualization of the estimated propagation paths of ham radio links established on the CW portion of the 40 m band during the Field Day experiment according to RBN records. The identified hams are marked by color. It is evident that hams were continuously transmitting during the entirety of the Field Day experiment.

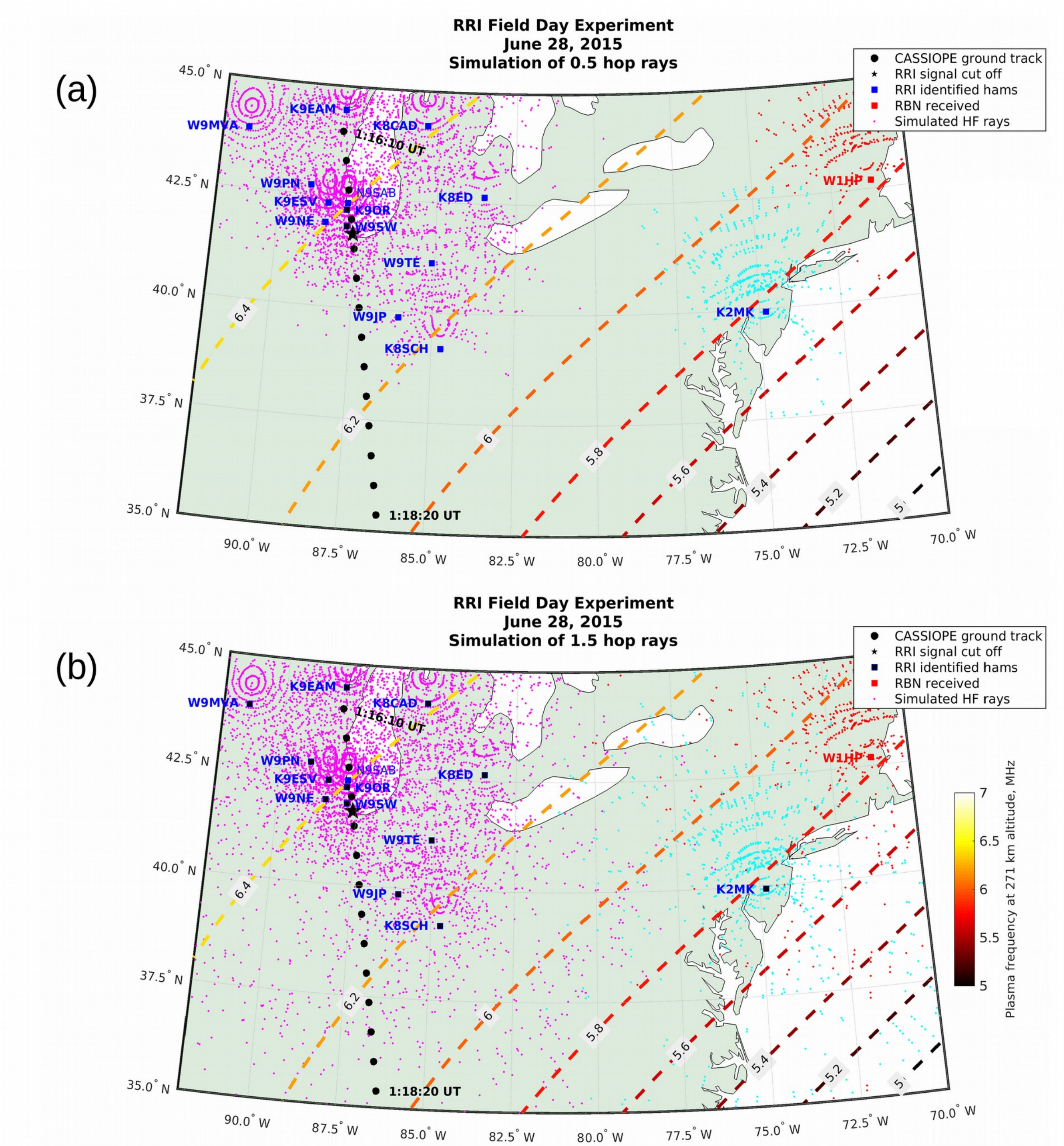

Figure 6: A reproduction of Figure 2 showing the results of the ray trace simulation. Points along the first half-hop of the rays (a) and the 0.5 and 1.5 hops (b), passing through CASSIOPE's altitude range during the experiment are plotted for all received Ham stations (magenta), K2MK (cyan), and W1HP (red).

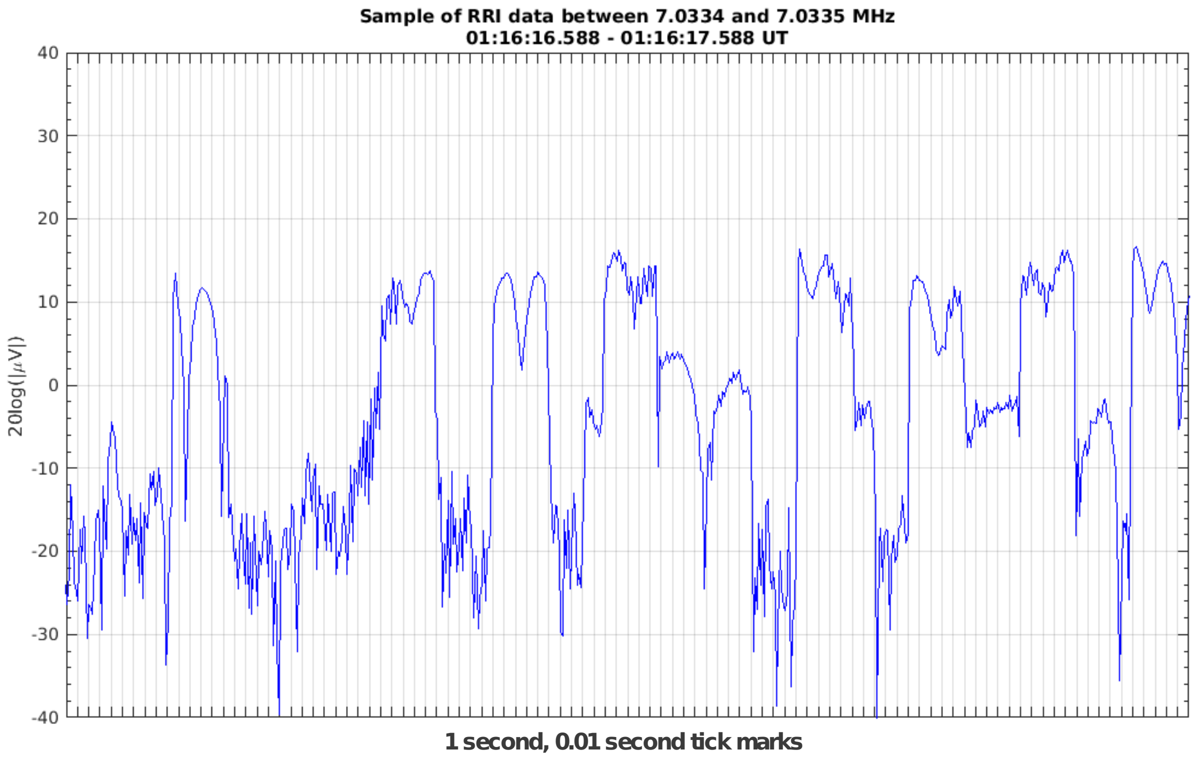

Figure 7: A one second excerpt of RRI's received signal between 7.0334 – 7.0335 MHz , corresponding to the 'ES' and part of 'V' in Figure 5. Each dot exhibits a significant doubled-peak modulation with a period on the order of 0.03 s, which is not attributed to an artificial source, e.g., transmitter quality.

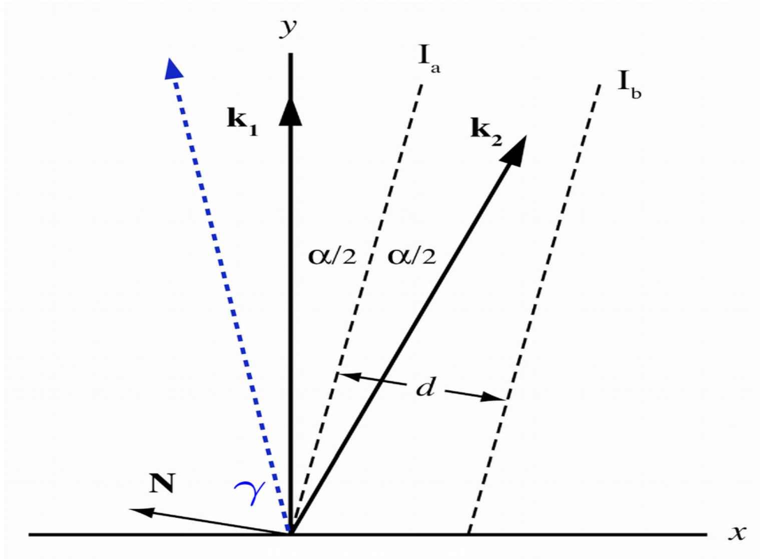

Figure 8: A reproduction of Figure 5 from James et al., [2006]. Planes of interference I_a and I_b are generated by the superposition of wave vectors k_1 and k_2.

827